Manuscript submitted to
AIMS' Journals
Volume **X**, Number **0X**, XX **200X**

Website: http://AIMsciences.org

pp. **X–XX**

COUPLING OF NON-LOCAL DRIVING BEHAVIOUR WITH FUNDAMENTAL DIAGRAMS

MICHAEL HERTY AND REINHARD ILLNER

M. Herty

RWTH Aachen University
Templergraben 55, D-52065 Aachen, Germany.

R. Illner

University of Victoria, Department of Mathematics and Statistics
PO Box 3060 STN CSC, Victoria, B.C., Canada V8W 3R4.

(Communicated by the associate editor name)

Abstract. We present an extended discussion of a macroscopic traffic flow model [18] which includes non-local and relaxation terms for vehicular traffic flow on unidirectional roads. The braking and acceleration forces are based on a behavioural model and on free flow dynamics. The latter are modelled by using different fundamental diagrams. Numerical investigations for different situations illustrate the properties of the mathematical model. In particular, the emergence of stop-and-go waves is observed for suitable parameter ranges.

1. **Motivation and Introduction.** We are concerned with refinements of the non-local traffic models previously introduced in [17] and [18], and this paper is a continuation of [18]. The studies done there show how non-local macroscopic models can be derived from kinetic models of Vlasov-type. They further contain a number of analytical and numerical investigations concerning the qualitative behaviour of solutions, such as the formation and propagation of traveling wave solutions, the impact of a local speed limit, and the origin of stop-and-go waves. In [22] the functional-differential equation arising for the propagation of a traveling braking wave is discussed as an interesting mathematical object in its own right.

The models are generalizations of the macroscopic model first suggested by Aw-Rascle [1] and Zhang [39]. In the form considered in [18] we observed that maximum principles are satisfied; while this is a pleasant feature from a mathematical point of view, it is rather unrealistic in real traffic. For example, consider a situation where traffic moves at a constant large speed u and a very high density ρ. The constant pair (ρ, u) will formally be a steady solution of the models from [18], but in reality drivers in such a situation would (because of safety concerns) make an effort to reduce density and speed and would slow down to this end. In versions of the Aw-Rascle model this is usually achieved by the inclusion of a relaxation term based on a fundamental diagram. In the simplest form, this means that in the absence of other stimuli drivers will brake or accelerate towards a comfortable

2000 *Mathematics Subject Classification.* Primary: 90B20; Secondary: 35L65.
Key words and phrases. Traffic Flow, Mathematical Modeling.

target speed $U^e(\rho)$, and the corresponding force term, to be used on the right hand side of the momentum transfer equation, is

$$\frac{1}{T_0}(U^e(\rho) - u).$$

Here T_0 is a characteristic relaxation time. The target speed $U^e(\rho)$ is also called equilibrium velocity–density relation. The associated equilibrium flux–density relation $\rho U^e(\rho) =: q(\rho)$ is called fundamental diagram.

Models of Aw-Rascle–Zhang type with these right hand sides have been studied extensively and with different versions of fundamental diagrams $\rho U^e(\rho)$. We refer to [2, 11, 27] for such research. Kimathi et al. [27] considered in particular the situation of three-phase traffic which emerges when fundamental diagrams are multi-valued, as suggested by B. Kerner [26]. Nonconcave fundamental diagrams for the Aw–Rascle–Zhang model have been studied e.g. by T. Li [30].

In this current work we consider the coupling of a variety of fundamental diagrams (including a multi-valued FD) with the non-local models introduced in [17, 18]. The full model will be introduced in Section 2. One of the features it displays is evaluation of the density and speed variables over stretches of the road which cover (in practice) 20 to 100 meters; if this is to be taken seriously, one has to include a discussion of the meaning to ρ and u. Such a discussion is often missing in papers on traffic, leading to confusion even among experts.

In continuum physics macroscopic variables emerge in what is usually referred to as the mean field limit; density, for example, is defined as the average number of particles (here cars) over a length Δx, such that the real number of particles in $[x, x + \Delta x]$ is $\rho(x)\Delta x$. For this interpretation is is certainly necessary that *many* particles fit in the reference interval; for cars, this means that Δx should have to be of the order of magnitude of at least hundreds of meters. The downside of such an interpretation would be that a macroscopic model would in principle be unable to resolve features which happen on shorter scales, or that emerging features on shorter scales have no meaning in the real world.

Fortunately, there is a second interpretation of the dependent variable ρ, u which does not face this problem. Simply define ρ to be the inverse to the distance to the lead car, or, a little more general, an inverse of the average of the distances to the leading cars within a visible window (and similarly for u). As was demonstrated convincingly in [2], this allows a reinterpretation of microscopic models in terms of macroscopic variables, and permits the use of the numerical tools available for nonlinear hyperbolic systems of equations. It is this interpretation which we will adopt for our purposes.

We conclude this introduction by a (very) brief review of other approaches to traffic modeling. Indeed, our models belong to only one class of possible models and ignore aspects of traffic such as variations in vehicle size and mass, driver behaviour, random fluctuations, etc. While it is possible to include such effects, our first priority here is simplicity in order to identify basic structures and explain arising phenomena.

Our model is a macroscopic model derived from a Fokker–Planck ansatz, see [24, 17, 19, 23]. Macroscopic models have been studied intensively in recent years and an incomplete list of references includes [1, 5, 6, 9, 10, 11, 12, 14, 20, 21, 28, 31, 33, 39]. Second order macroscopic models use equations similar to fluid dynamics models to describe the evolution of traffic density and velocity profiles. In

contrast, microscopic models keep track of individual drivers and their interactions in order to explain traffic phenomena. Some references on microscopic models are [7, 8, 15, 16, 26, 38, 34, 35]. Microscopic models can take the form of systems of ordinary differential-delay equations, or of discretized versions such as cellular automata. These models have been extended to include stoachstic effects, see e.g., [32], [36, 37]. Finally, there is a class of kinetic models of Enskog–type which relates to microscopic and macroscopic models, see e.g. [25].

2. **Modelling.**

2.1. **Parameters and Notation.** Throughout this paper x, t will denote position (on the road) and time.
$\rho = \rho(x,t), u = u(x,t)$ denote the macroscopic density and the macroscopic (average) speed of cars on a highway (freeway) lane. Lane changing is included in the sense that certain types of fundamental diagrams (to be introduced later) emerge only when lane changes are possible and occur.

The non-local model includes three parameters which exist in real traffic: A minimum safety distance $H > 0$ of the order of magnitude of 8 meters (measured from the front of a car to the front of the lead car; this applies in moving traffic and is larger than the minimum distance in standing traffic, which is the inverse of the maximal density), a characteristic reaction time $T > 0$, which multiplies the driver's speed such that $[x, x + H + Tu]$ is the window from which a driver at x and moving with speed u draws (visual) information, and finally a reaction time $\tau > 0$. T should be thought of as being about 2 seconds, $\tau \leq 1$ second. At a typical speed of 15 meters per second, the window would then be 38 meters long.

With u, ρ taken at (x,t) we introduce the abbreviations

$$u^X(x,t) = \inf_{\sigma \in [x, x+H+Tu]} u(\sigma, t-\tau), \tag{1}$$

(the smallest speed observed in the visible window)

$$\rho^+(x,t) = \sup_{\sigma \in [x, x+H+Tu]} \rho(\sigma, t-\tau), \tag{2}$$

$$u^Y(x,t) = \sup_{\sigma \in [x, x+H+Tu]} u(\sigma, t-\tau), \tag{3}$$

and

$$\rho^-(x,t) = \inf_{\sigma \in [x, x+H+Tu]} \rho(\sigma, t-\tau). \tag{4}$$

2.2. **The Fundamental Diagram. Braking and Acceleration Forces.** Drivers are assumed to have a target speed in mind associated with a certain density, and if no other inputs are active, they will brake or accelerate towards this target speed. We assert that this behaviour produces a force F given by relaxation towards the equilibrium velocity–density relation $U^e(\rho)$. In the simplest case

$$F = \frac{1}{T_0}\left(U^e(\rho) - u\right). \tag{5}$$

As indicated earlier, U^e may be a multi-valued function. This is best expressed as an additional dependence $U^e(\rho, u)$. We will provide and use an example below; the structure of a multi-valued U^e is best understood from a graphical representation (see Figure 1).

We emphasize that the force F is active only if no other (overriding) forces apply. Such forces are active if the driver is in a "compelling" braking or acceleration

situation. The word "compelling" here means that the driver realizes the need to brake or accelerate; to this end we introduce one more parameter $\epsilon \geq 0$, a (low) threshold for reaction. The force term which is active on the right hand side of the speed (or momentum transfer) equation is then defined for all possible cases, as follows (we distinguish cases A to D):

A.

$$\text{If} \quad u - u^X > \epsilon \quad \text{let} \quad B = \min\{c_1 \left(\frac{\rho_{max}\rho^+}{\rho_{max} - \rho^+} \right) (u^X - u), F\} \tag{6}$$

This means that braking dominates, and the braking force is the stronger of the two given by the speed relative to u^X and the one given by the equilibrium velocity. The factor multiplying $u^X - u$ is sometimes called "speed adaptation coefficient" (see [27] and the references therein). It has been introduced in [3] for the Aw–Rascle model to avoid inconsistencies concerning the maximal density. The precise form is not important but it needs to be guaranteed that the factor diverges to ∞ as ρ^+ approaches the possible maximum.

B.

$$\text{If} \quad u - u^X \leq \epsilon \quad \text{and} \quad F < 0 \quad \text{let} \quad B = F. \tag{7}$$

This means that braking still dominates if the equilibrium velocity calls for braking, even if the relative speed is close to 0 or negative.

C.

$$\text{If} \quad u - u^X \leq \epsilon, \ F \geq 0 \quad \text{and} \quad u^Y - u > \epsilon$$

apply an acceleration force A be defined by

$$A = \max\{c_2(\rho_{max} - \rho^-)(u^Y - u), F\} \tag{8}$$

This is an acceleration scenario, and we accelerate by either the force suggested by the speed relative to u^Y, or by the equilibrium velocity. Notice that the speed adaptation coefficient is now taken as a decreasing function of ρ^- – higher densities should imply reduced acceleration.

D. And finally, if none of the above apply, the force is simply

$$F = F(\rho, u) = \frac{1}{T_0} \left(U^e(\rho, u) - u \right). \tag{9}$$

– the equilibrium velocity–density relation is the only remaining input.

In the following numerical simulations we allow different $U^e(\rho)$ and depicte in Figure 1 some choices explained in detail below.

I The Greenshields model [13], which we include here for completeness, with the two parameters maximal velocity $v_{\max}$ and maximal density $\rho_{\max}$, is given by

$$U^{eq}(\rho) = v_{\max}(\rho - \rho_{\max}). \tag{10}$$

We conducted but do for conciseness not include numerical experiments.

II A more realistic nonlinear equilibrium velocity is

$$U^e(\rho) = v_{\max} \left(1 - \frac{1}{\pi} \left(atan \left(30\pi \left(\rho - \frac{\rho_{\max}}{3} \right) \right) + \frac{\pi}{2} \right) \right). \tag{11}$$

The shape of this function is similar to the examples considered in [25, 27]. It is a better match to traffic data due to the small transition zone between free flow $\rho < \frac{\rho_{\max}}{3}$ and congested traffic.

III An example of equilibrium velocity relation attaining multiple values in the region $I := [\rho_-, \rho_+]$ given by

$$U^e(\rho,u) = \begin{pmatrix} U^e\left(\rho + \frac{\rho_{\max}}{3} - \frac{5}{4}\rho_+\right) & u > u^*(\rho), \rho \in I \text{ or } \rho < \rho_- \\ u^*(\rho) & u = u^*(\rho), \rho \in I \\ U^e\left(\rho + \frac{\rho_{\max}}{3} - \frac{3}{4}\rho_-\right) & u < u^*(\rho), \rho \in I \text{ or } \rho > \rho_+ \end{pmatrix} \tag{12}$$

Here, we choose $U^e(\rho)$ given by (11). The other parameters are as follows $\rho_\pm = \frac{\rho_{\max}}{3} \pm \frac{1}{20}\rho_{\max}$, $u^*(\rho) = \frac{u_+ - u_-}{\rho_+ - \rho_-}(\rho - \rho_-) + u_-$ for $u_- = U^e(\frac{1}{2}\rho_-)$ and $u_+ = U^e(-\frac{1}{4}\rho_-)$. Similar diagrams were discussed in [27], where is was shown how these mutli–valued diagrams help to explain stop–and–go waves. It has been argued [27, 25]that the existence of multi–valued functions is due to the possibility of cars changing lanes. In [24] a kinetic multi–lane model for vehicular flow has been proposed. By moment approximations single lane models with multi–valued functions $U^e(\rho)$ could be obtained due to the lane changing terms.

These definitions define forces for all possible scenarios as a functional of the (delayed, non-local) traffic state. If we write R for the functional defined by cases A to D , our traffic model is in short

$$\frac{\partial}{\partial t}\rho + \frac{\partial}{\partial x}(\rho u) = 0 \tag{13}$$

and

$$\frac{\partial}{\partial t}u + u\frac{\partial}{\partial x}u = R \tag{14}$$

To summarize we have for fixed parameters ϵ and τ the functional $R = R(\rho^-, \rho^+, \rho, u^X, u^Y, u)$ given by either (6), (7), (8) or (9) depending on the size of the relative velocity $u - u^X$ and $u - u^Y$ and the sign of F. Further, $F = F(\rho, u)$ is given by either equation (11) or (12).

Notice that the B which arises in braking scenarios is by construction always nonpositive. The definition of the force term R is asymmetric in preference of braking, a reasonable construction in view of safety considerations.

3. **Numerical simulations.** The system of balance laws (13-14) is solved numerically by a first–order finite volume method on a uniform grid with N_x grid points in space. Prior to discretization, the momentum equation is rewritten in the conservative variable (ρu). We then apply a first–order time–splitting procedure and obtain a system of conservation laws and the ordinary differential equation

$$\frac{d}{dt}\rho = 0, \ \frac{d}{dt}u = R.$$

The transport part are then the well–known equations of pressure-less gas dynamics. A Godunov scheme in the conservative variables $(\rho, \rho u)$ for these equations can be found in [29]. We use precisely this scheme for discretization of the transport part. Time and spatial discretization are chosen such that the CFL condition is satisfied. Alternative discretizations can be found in [4] or the references therein. The source term R depends on local and nonlocal terms and we may write

$$R = R(\rho^-, \rho^+, \rho, u^X, u^Y, u).$$

Depending on the actions of braking, acceleration and equilibrium flow the dependence on the u variable is either $u^X - u, u^Y - u$ or $U^{eq}(\rho) - u$. In space we discretize

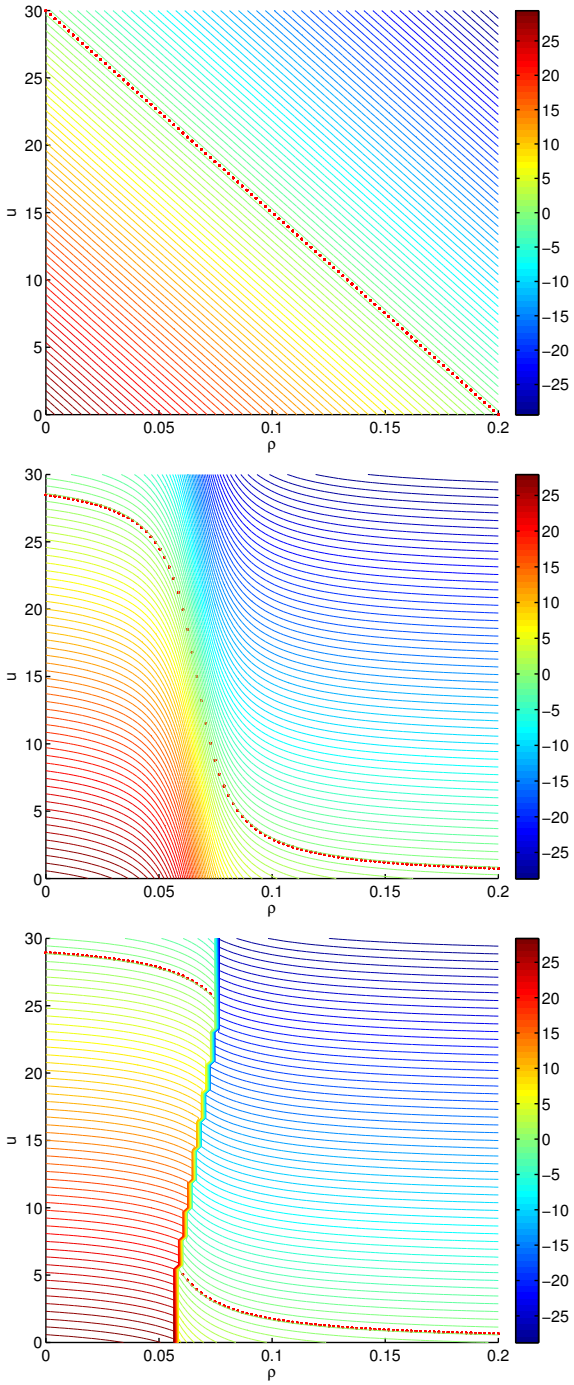

FIGURE 1. Equilibrium velocities U^e and $U^e(\rho, u)$ (dotted red line) given by (10)-(12), respectively. Also shown are the contour lines of the acting forces $U^e(\rho, u) - u$.

all arguments of R at at the center of each cell with piecewise constant reconstruction of ρ and u. To compute u^X we simply use the nearest neighbours and linear interpolation. In the splitting the ordinary differential equation is solved by a mixture of an implicit and explicit Euler method. To be more precise, the discretization at time t_n and location x_i and for $u_{n,i} = u(t_n, x_i)$ is

$$u_{n+1,i} = u_{n,i} + \Delta t R(\rho^-_{n,i_1}, \rho^+_{n,i_2}, \rho_{n,i}, u^X_{n,i_3}, u^Y_{n,i_4}, u_{n+1,i}).$$

Here, the index i_j for $j = 1, \ldots, 4$ is computed according to equations (1)-(4). The discretization is only implicit in the variable u. Higher–order spatial and temporal discretizations could also be used in order to solve the equations numerically. However, since the problem is one–dimensional in space the computational time even on very fine grids is within minutes. If not stated otherwise we set up a "circular" road (using periodic boundary conditions) and use parameter values as given in table 1. Initial data are prescribed as discussed below. All computations have been performed on a 2.4 GHz Intel Core 2 Duo.

3.1. **Parameters.** The source term R in the equation (14) contains a number of parameters. The safety distance is about twice the length of a car, giving rise to a maximal density of $\rho_{\max} = 0.2$. This means that 5 meters is the average length of a car. The anticipation time of the drivers is two seconds, which, at maximal speed, yields an additional look-ahead distance of 60 m. The maximal velocity is set at 108 km/h — a model for highway traffic in the USA and Canada. For the reaction time of the drivers we choose $\tau = 0.5sec$. We also present results with zero reaction time. The weights c_1, c_2, c_3 for braking, acceleration and free flow traffic are a priori unknown. We assume that the drivers have a tendency to brake harder than to accelerate, or to react to free flow traffic. We simulate traffic for 20 second periods on a strip of the highway of length 4 km. The mesh consists of 20,000 points which means one grid point per 20 cm. All parameters are summarized in Table 1.

In contrast to the simulations in [18] there is no additional trigger involved in the simulations.

Name	Description	Value	Unit
H	safety distance	10	m
T	anticipation time	2	s
$\rho_{\max}$	maximal density	0.2	$1/m$
$u_{\max}$	maximal velocity	30	m/s
τ	reaction time	$\in \{0, \frac{1}{2}\}$	s
c_1	weight (braking)	16	$1/s$
c_2	weight (acceleration)	3	$1/s$
$c_3 \equiv \frac{1}{T_0}$	weight (equilibrium)	0.05	$1/(ms)$
ϵ	velocity threshold	0.15	m/s
$L_{\max}$	length of the road	4,000	m
L_{res}	length of speed limit	200	m
u_{lim}	speed limit velocity	15	m/s
$T_{\max}$	time horizon of the simulation	20	s
N_x	gridpoints in spatial domain	20,000	

TABLE 1. Parameters of the numerical integrations

3.2. **A lane reduction.** We next study the effect of a lane reduction on the evolution of the downstream traffic flow. This is modelled by increasing the initially constant density of $\rho_0 = 0.2\rho_{\max}$ to $0.3\rho_{\max}$ on a strip of length 40% of the road starting at $x = 2000m$. The initial transition from the lower to higher density is smooth. The smooth connection on a length of $10m$ is obtained by suitable adjusted atan function. The initial velocity is always the equilibrium velocity corresponding to the lower density. Hence, in this setup the cars within the lane reduction area are moving uncomfortably fast (as defined by the function $U^e(\rho)$) and start braking. Due to the length of the lane reduction the effects of acceleration at the exit point of the lane reduction area and the braking in the beginning do not interact. In Figure 2 we present density and velocity at time $T_{\max}$ using different fundamental diagrams in the simulation and zero reaction time. In Figure 3 and Figure 4 the same result using a reaction time of $\tau = \frac{1}{2}$ are presented. A contour plot of the full solution over space and time for choice (12) and a reaction time $\tau = \frac{1}{2}$ is given in Figure 5.

We observe finite oscillations in the density. Those are expected and they do not reach or exceed the maximal density in the simulation. They arise from changes in the velocity profile. Due to the pressureless gas dynamics model such oscillations lead to oscillations in the density. The frequency of this oscillations is related to the non–local effect in the equation. In particular, in Figure 4 the occurrence of stop–and–go waves with wavelength of about 50 m are observed.

We conducted but do not present the same experiments with reaction time $\tau = 1$. In this case the density exceeded ρ_{max}, at which point the model loses its meaning (the interpretation would be that an accident has happened).

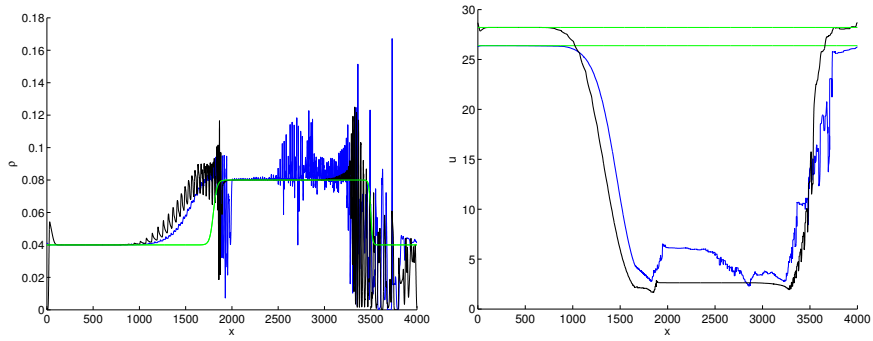

FIGURE 2. Density and velocity at time $T_{\max}$ for initial data corresponding to a lane reduction and constant initial velocity. Different colors correspond to the different choices of $U^e(\rho)$ used in the simulation: blue and black correspond to equations (11) and (12), respectively. Initial data is depicted in green. Reaction time is zero. Left: density, right: velocity .

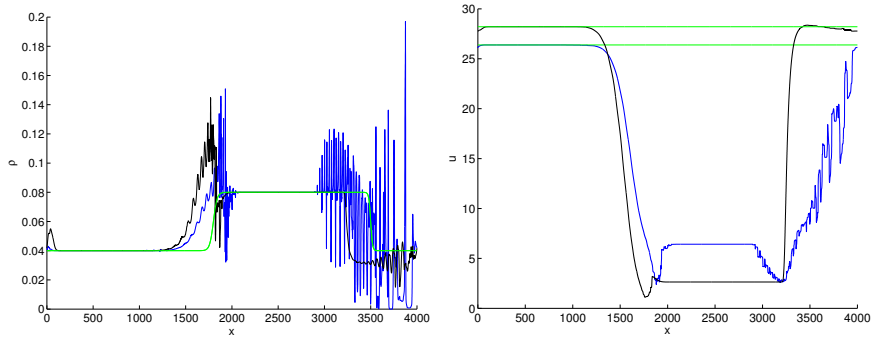

FIGURE 3. Density and velocity at time $T_{\max}$ for initial data corresponding to a lane reduction and constant initial velocity. Different colors correspond to the different choices of $U^e(\rho)$ used in the simulation: blue and black correspond to equations (11) and (12), respectively. Initial data is depicted in green. Reaction time is $\tau = \frac{1}{2}$. Left: density, right: velocity.

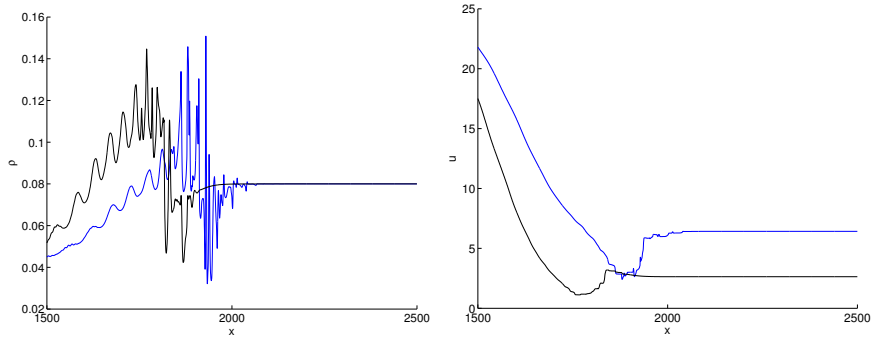

FIGURE 4. Density and velocity at time $T_{\max}$ for initial data corresponding to a lane reduction and constant initial velocity. Different colors correspond to the different choices of $U^e(\rho)$ used in the simulation: blue and black correspond to the equations (11) and (12), respectively. Reaction time is $\tau = \frac{1}{2}$. Left: density, right: velocity.

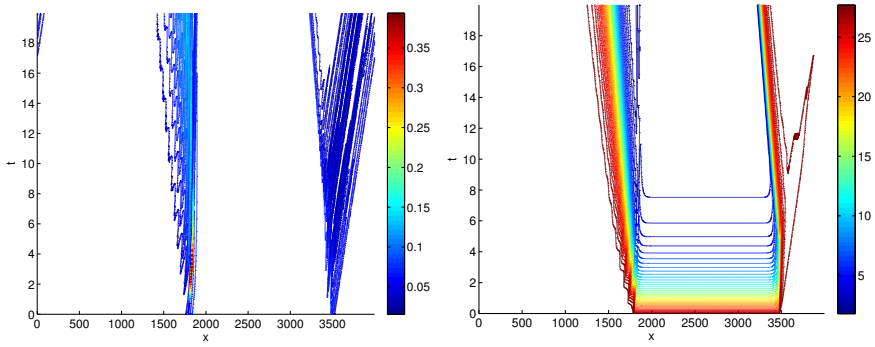

FIGURE 5. Density and velocity at time $T_{\max}$ for initial data corresponding to a lane reduction and constant initial velocity. Equilibrium velocity (12) and a reaction time of $\tau = \frac{1}{2}$ were used. Left: density, right: velocity.

3.3. **The effect of a speed limit.** As in [18] we finally consider a speed limit. In order to treat the effect of the speed limit on the dynamics we proceed as in [18, 4.2.2]. We assume the speed limit is active in an interval I of length $L_{res} = 200m$ centered at $x = 2000m$. The velocity within the speed limit is $u_{lim} = 15m/s$. In the area of the speed limit the braking term is modified as follows:

$$B = \min\{c_1 \left(\frac{\rho_{max}\rho^+}{\rho_{max} - \rho^+} \right) (u - u^{lim}), F\} \text{ if } x \in I \text{ and } u > u_{lim}.$$

No further changes are applied to the model. We start with initial constant densities in the range of $10\% - 40\%$ of the maximal density and constant velocity of $U^e(\rho)$. As always, we study the arising wave patterns. The solution is presented in Figure 6 and Figure 7 for the case of a reaction time of $\tau = \frac{1}{2}$ and equilibrium velocities (11) and (12), respectively. The area of the speed limit is depicted by red dots. Due to the different shapes of $U^e(\rho)$ different densities give rise to different initial velocities. Therefore, the braking patterns are more pronounced in Figure 7. As in previous situations we observe a step-like behaviour in the speed profile and high oscillations in the density evolution. For the intermediate density and equation (12) we observe a density equal to $\rho_{\max}$ which is the maximal density. As mentioned earlier, this means that a road accident has occurred and the model is not valid any more. In Figure 6 this case occured at time $T^* = 1.08$ and $T^* = 1.77$ for the medium and large density, respectively. In Figure 7 this happened at time $T^* = 2.75$ and $T^* = 1.77$ for medium and large density, respectively. In the case of zero reaction time or low initial density there is no accident observed in the simulation. The results for zero reaction time are given in Figure 8 and Figure 9, respectively.

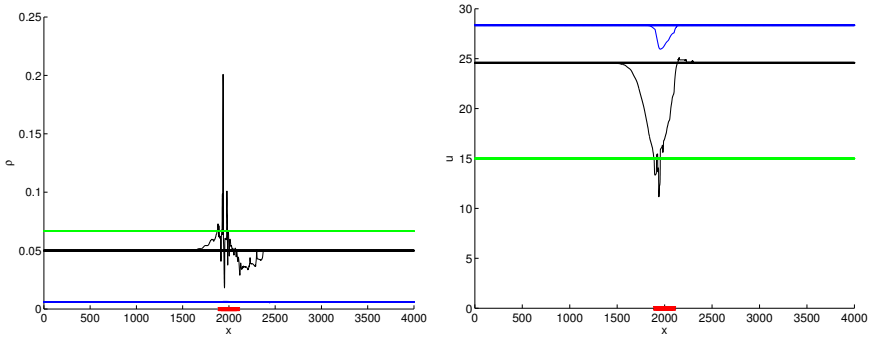

FIGURE 6. Density and velocity at time T^* where either $T^* = T_{\max}$ or at time T when the density exceeds the maximal density $\rho_{\max}$. Different initial densities correspond to different colors with blue being light traffic, black intermediate traffic and green moderately dense traffic. The speed limit of u_{lim} is imposed within the red area. Equilibrium velocity (11) and a reaction time of $\tau = \frac{1}{2}$ are used in the simulations. Left: density, right: velocity.

4. **Conclusions.** We presented a refined model of traffic flow, in which non-local braking and acceleration terms are augmented by forces given by an equilibrium

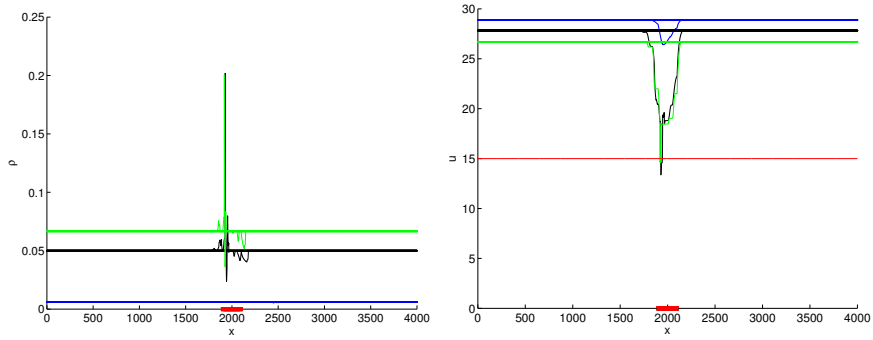

FIGURE 7. Density and velocity at time T^* where either $T^* = T_{\max}$ or at time T when the density exceeds the maximal density $\rho_{\max}$. Different initial densities correspond to different colors with blue being light traffic, black intermediate traffic and green moderately dense traffic. The speed limit of u_{lim} is imposed within the red area. Equilibrium velocity (12) and a reaction time of $\tau = \frac{1}{2}$ are used in the simulations. Left: density, right: velocity.

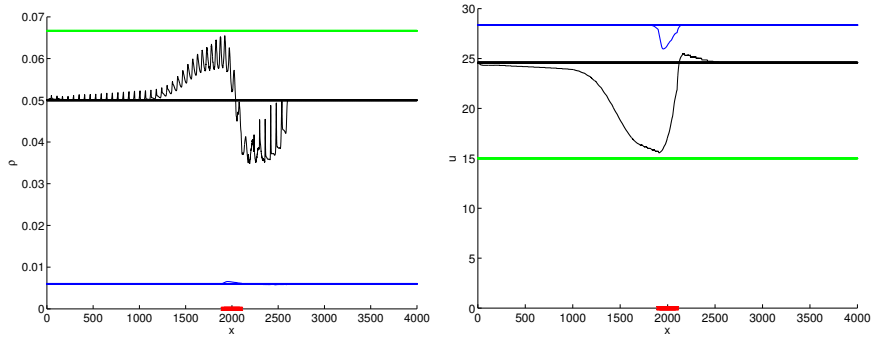

FIGURE 8. Density and velocity at time $T_{\max}$. Different initial densities correspond to different colors with blue being light traffic, black intermediate traffic and green moderately dense traffic. The speed limit of u_{lim} is imposed within the red area. Equilibrium velocity (11) and a reaction time of $\tau = 0$ are used in the simulations. Left: density, right: velocity.

velocity. By two numerical experiments (lane reduction and implementation of a local speed limit) we indicate the following features, consistent with expectations.

- Non–locality has a significant effect, generating all by itself traffic waves of realistic wave lengths.
- These effects are amplified if traffic densities are in a range where the fundamental diagram has steep slope, or worse, is multi-valued.
- Larger individual reaction times have a destabilizing effect, to the point where there are collisions.

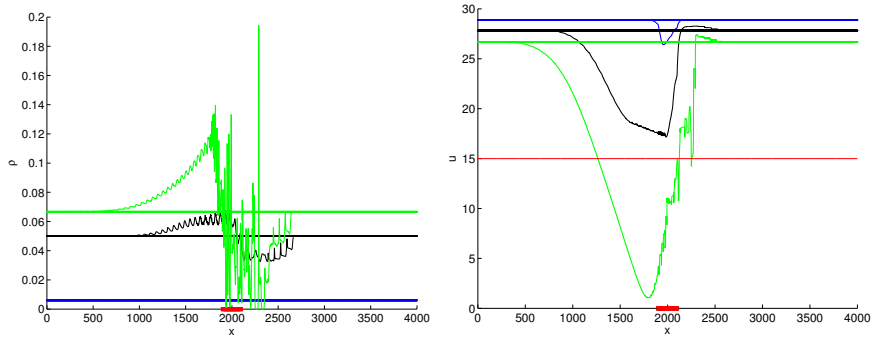

FIGURE 9. Density and velocity at time $T_{\max}$. Different initial densities correspond to different colors with blue being light traffic, black intermediate traffic and green moderately dense traffic. The speed limit of u_{lim} is imposed within the red area. Equilibrium velocity (12) and a reaction time of $\tau = 0$ are used in the simulations. Left: density, right: velocity.

Acknowledgments. This work has been supported by HE5386/8-1, DAAD 54365630, and by Discovery grant No. 7847 of the Natural Sciences and Engineering Research Council of Canada.

REFERENCES

[1] A. Aw and M. Rascle, *Resurrection of "second order" models of traffic flow.*, SIAM J. Appl. Math., 60 (2000), pp. 916–938.
[2] A. Aw, A. Klar, Th. Materne and M. Rascle,*Derivation of continuum traffic flow models from microscopic follow-the-leader models.*, SIAM J. Appl. Math., 63 (2002), pp. 259–278.
[3] F. Berthelin, P. Degond, M. Delitala, and M. Rascle, *A model for the formation and evolution of traffic jams*, Arch. Ration. Mech. Anal., 187 (2008), pp. 185–220.
[4] A. Chertock, A. Kurganov, Y. Rykov, *A New Sticky Particle Method for Pressureless Gas Dynamics*, SIAM J. on Numerical Analysis, Vol. 45 (2007), pp. 2408–2441
[5] G. M. Coclite, M. Garavello and B. Piccoli, *Traffic flow on a road network*, SIAM J. Math. Anal., 36 (2005), pp. 1862–1886.
[6] C. F. Daganzo, *The cell transmission model : A dynamic representation of highway traffic consistent with the hydrodynamic theory*, Transp. Res. B, 28 (1994), pp. 269-287.
[7] I. Gasser, T. Seidel, G. Sirito, and B. Werner, *Bifurcation Analysis of a Class of Car Following Traffic Models II: Variable Reaction Times and Agressive Drivers*, Bulletin of the Institute of Mathematics, Academica Sinica (New Series), 2 (2007), pp. 587–607.
[8] I. Gasser, G. Sirito, and B. Werner, *Bifurcation analysis of a class of 'car following' traffic models.*, Physica D, 197 (2004), pp. 222–241.
[9] J. Greenberg, *Extensions and amplifications of a traffic model of Aw and Rascle.*, SIAM J. Appl. Math., 62 (2001), pp. 729–745.
[10] ———, *Congestion redux.*, SIAM J. Appl. Math., 64 (2004), pp. 1175–1185.
[11] ———, *Traffic congestion – an instability in a hyperbolic system*, Bulletin of the Institute of Mathematics, Academica Sinica (New Series), 2 (2007), pp. 123–138.
[12] J. Greenberg, A. Klar, and M. Rascle, *Congestion on multilane highways.*, SIAM J. Appl. Math., 63 (2003), pp. 818–833.
[13] B. D. Greenshields, *A study of traffic capacity*, Proc. Highway Res., 14 (1935), pp. 448–477.
[14] R. Herman, I. Prigogine, *A two-fluid approach to twon traffic*, Science, Vol. 204 (1979), oo. 148-151

[15] D. Helbing, *Traffic dynamics. New physical concepts of modelling. (Verkehrsdynamik. Neue physikalische Modellierungskonzepte.)*, Berlin: Springer. xii, 308 p. DM 128.00; öS 934.40; sFr 113.00 , 1997.
[16] D. Helbing, A. Hennecke, V. Shvetsov, and M. Treiber, *Micro- and macro-simulation of freeway traffic.*, Math. Comput. Modelling, 35 (2002), pp. 517–547.
[17] M. Herty, R. Illner, *On stop-and-go waves in dense traffic.*, Kinetic and Related Models 1(3)(2008), pp. 437-452.
[18] M. Herty, R. Illner, *Analytical and Numerical Investigations of Refined Macroscopic Traffic Flow Models*, Kinetic and Related Models, 3(2) (2010), pp. 311 333.
[19] M. Herty, R. Illner, A. Klar, and V. Panferov, *Qualitative properties of solutions to systems of Fokker-Planck equations for multilane traffic flow.*, Transp. Theory Stat. Phys., 35 (2006), pp. 31–54.
[20] M. Herty and A. Klar, *Modelling, simulation and optimization of traffic flow networks*, SIAM J. Sci. Comp., 25 (2003), pp. 1066-1087.
[21] M. Herty and M. Rascle, *Coupling conditions for a class of second-order models for traffic flow*, SIAM J. Math. Anal., 38 (2006), pp. 595-616.
[22] R. Illner and G. McGregor, *On a functional-differential equation arising from a traffic flow model*, SIAM J. Appl. Math. 72 (2012), pp. 623-645.
[23] R. Illner, C. Kirchner, and R. Pinnau, *A derivation of the Aw–Rascle traffic models from Fokker-Planck type kinetic models*, Quarterly Appl. Math., 67(1) (2009), pp. 39–45
[24] R. Illner, A. Klar, and T. Materne, *Vlasov-Fokker-Planck models for multilane traffic flow.*, Commun. Math. Sci., 1 (2003), pp. 1–12.
[25] A. Klar, R .Wegener, *A hierarchy of models for multilane vehicular traffic. I. Modeling.*, SIAM J. Appl. Math., Vol. 3 (1999), pp. 983–1001
[26] B. Kerner, *The Physics of traffic*, Springer, Berlin, 2004.
[27] M. E. M. Kimathi, *Mathematical Models for 3-Phase Traffic Flow Theory.*, Ph. D. Thesis, Kaiserslautern 2012
[28] J. P. Lebacque and M. Khoshyaran, *First–order macroscopic traffic flow models for networks in the context of dynamic assignment*, Transportation Planning and Applied Optimization, Vol. 64 (2004), pp. 119–140
[29] R. LeVeque, *The dynamics of pressureless dust clouds and delta waves*, Journal Hyperbolic Differential Equations, Vol. 1 (2004), pp. 315–327
[30] T. Li, *Global Solutions of Nonconcave Hyperbolic Conservation Laws with Relaxation Arising From Traffic Flow*, J. Diff. Eqn., Vol. 190 (2003), pp. 131–149
[31] M. Lighthill and J. Whitham, *On kinematic waves*, Proc. Roy. Soc. London Ser. A, 229 (1955), pp. 281–345.
[32] E. Ben-Naim, P. L. Krapinsky, S. Redner, *Kinetics of clustering in traffic flows*, Physical Rev. E 50(2), (1994) pp. 822–829.
[33] P. I. Richards, *Shock waves on the highway*, Oper. Res., 4 (1956), pp. 42–51.
[34] L. Santen, A. Schadschneider, M. Schreckenberg, *Towards a realistic microscopic description of highway traffic*, J. Phys A, Vol. 33, (2000), pp. 477–485
[35] S. Marinosson, R. Chrobok, A. Pottmeier, J. Wahle, M. Schreckenberg, *Simulation framework for the autobahn traffic in North Rhine-Westphalia*, Cellular automata 315–324, Lecture Notes in Comput. Sci., 2493, Springer, Berlin (2002)
[36] T. Alperovich, A. Sopasakis, *Stochastic description of traffic flow*, J. Stat. Phys., Vol. 133 (2008), pp. 1083-1105
[37] A. Sopasakis, M.A. Katsoulakis, *Stochastic modeling and simulation of traffic flow: asymmetric single exclusion process with Arrhenius look-ahead dynamics*, SIAM J. Appl. Math., Vol. 66 (2006), pp. 921-944.
[38] M. Treiber and D. Helbing, *Macroscopic simulation of widely scattered synchronized traffic states.*, J. Phys. A, Math. Gen., (1999).
[39] H. M. Zhang, *A non–equilibrium traffic model devoid of gas–like behavior*, Tans. Res. B, Vol. 36 (2002), pp. 275–290

Received xxxx 20xx; revised xxxx 20xx.

E-mail address: herty@igpm.rwth-aachen.de
E-mail address: rillner@math.uvic.ca